

PAPER • OPEN ACCESS

## Ammonia heat pumps for district heating: thermo-economic optimization analysis based on evaporator geometry for either direct expansion or chilled water configurations

To cite this article: A F Passarelli *et al* 2023 *J. Phys.: Conf. Ser.* **2648** 012093

View the [article online](#) for updates and enhancements.

You may also like

- [Implementation of energy conservation in a commercial building using BEM and sub-metering technology](#)

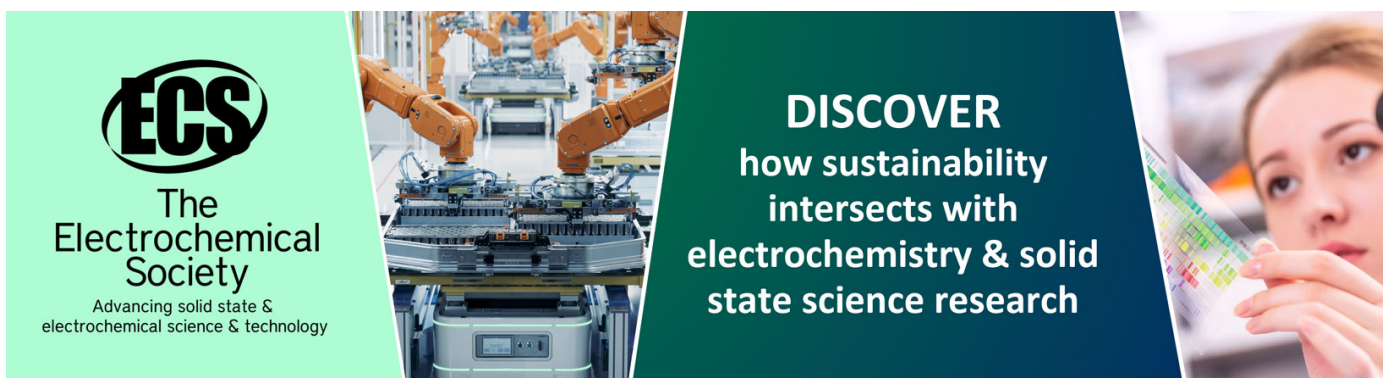
Chao Wang, Zhenqian Chen, Zhichao Tian et al.

- [Modeling and optimization for the smart operation of a central chilled water system in a high-rise building](#)

Hai Wang, Hua Meng, Ran Ju et al.

- [Investigation on the performance of the chilled water system with the key sensor fault](#)

J N Liu, G N Li, Y P Hu et al.



**ECS**  
The  
Electrochemical  
Society  
Advancing solid state &  
electrochemical science & technology

**DISCOVER**  
how sustainability  
intersects with  
electrochemistry & solid  
state science research

# Ammonia heat pumps for district heating: thermo-economic optimization analysis based on evaporator geometry for either direct expansion or chilled water configurations

A F Passarelli<sup>1</sup>, L Viscito<sup>1</sup>, U Merlo<sup>2</sup>, S Filippini<sup>2</sup>, A W Mauro<sup>1</sup>

<sup>1</sup> Department of Industrial Engineering, Università degli Studi di Napoli – Federico II, P.le Tecchio, 80, 80125 Naples, Italy

<sup>2</sup> LU-VE Group, Uboldo, 21040, Italy

Corresponding author: wmauro@unina.it

**Abstract.** Electric heat pumps are recognized as a key technology for decarbonization and have received increasing policy support in several countries over the last few years. These devices offer a highly efficient form of electric heating and could make an important contribution to the transition to a low carbon future, especially in case of district heating systems. Within this context, this paper presents a thermo-economic optimization analysis of a 7.35 MW electric heat pump system employed for district heating purposes and using ammonia as working fluid. The implemented code gathers multiple sub-models calibrated ad-hoc from real data or manufacturers' datasheets. The heat exchangers are simulated by considering phenomenological equations and well-known heat transfer coefficient and pressure drop prediction methods. The optimization analysis is performed at constant condensation temperature that guarantees in/out hot water temperatures of 30/62 °C and is focused on the matching between compressor and evaporator heat exchanger, by considering either a direct expansion system or a chilled water heat pump. Both the coefficient of performance (COP) and the set-up costs are considered as optimization performance indicators for the construction of the Pareto front.

## 1. Introduction

According to the latest data [1], almost half of the energy demand for buildings is related to space and water heating and a large part of it is obtained through fuel combustion, in particular natural gas. Indeed, about 50% of GHG emissions from energy use in buildings in the EU is related to fossil fuels [2].

In order to meet the net-zero objective, it is crucial to decarbonize also the heating sector through the massive diffusion of heat pumps systems driven by energy from renewable sources or nuclear. A key role to achieve this objective can be played by district heat pump systems, allowing the use of different heat sources with different plant solutions [3] and working fluids [4].

Therefore, it is important to carry out thermo-economic analyses to find out the optimal solution, in terms of efficiency and set-up costs. The case study proposed in this paper is related to a 7.35 MW electric heat pump system located in Denmark, using ammonia as working fluid, employed for district heating hot water production from 30 °C to 62 °C.

Since different plant solutions can be employed for this application, and given that a specific plant solution may have several configurations in terms of heat exchangers elementary geometry, a thermo-



economic optimization analysis is needed to firstly understand what is the best configuration for the specific solution analysed and then which plant configuration better copes with the objectives.

Therefore, this paper will focus on the optimization and comparison of two different plant solutions: direct expansion and chilled water configuration. The analysis will be performed considering the running costs for three different electricity prices scenarios and the difference in set-up costs related only to the components that differs between the two options.

## 2. Thermodynamic cycles description

The two possible heat pump plant schemes are presented in figure 1 with their relative T-s diagram shown in figure 2.

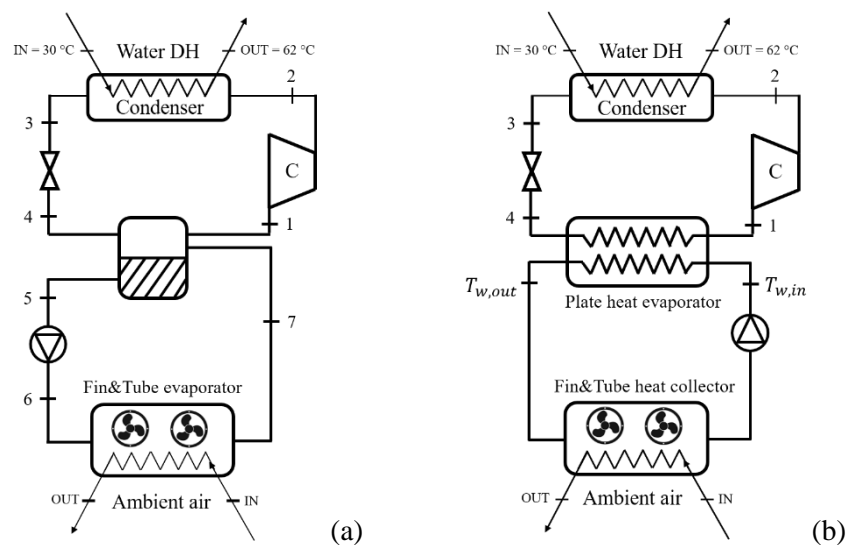


**Figure 1.** Direct expansion (a) and chilled water configuration (b) scheme.

The two layouts shown have some components in common, such as the condenser, the one stage liquid-cooled compressor and the expansion valve, whereas there are some differences for the low-pressure zone. For the direct expansion system, the saturated vapor goes into a liquid receiver where the liquid phase continues to the evaporators, whereas the vapor phase goes to the suction line.

Fin and tube evaporators allow the heat transfer with ambient air and the refrigerant comes back to the liquid receiver with an intermediate vapor quality condition.

Instead, for the chilled water configuration, the evaporation phase with a fixed superheating grade occurs in a plate heat exchanger working with a glycol/water mixture as secondary fluid that closes its loop passing through fin and tube heat exchangers working as heat collector from ambient air.

## 3. Modelling

### 3.1. Thermodynamic cycle modelling

The thermodynamic cycle is evaluated starting from the ambient conditions in terms of temperature and relative humidity, to obtain the evaporation temperature once fixed all the heat exchangers pinch points and secondary fluid temperature profiles, assuming a fixed condensation phase and subcooling grade with the presence of superheating only for chilled water configuration.

Through these input parameters it is possible to calculate all the key thermodynamic points shown in figure 2, including the mass flow rate and the thermal powers, once the condensing power output is fixed. The compressor discharge condition has been evaluated using a general correlation between pressure ratio  $\beta$  and global efficiency  $\eta_c$  for this kind of devices, obtained as follows [5] [6]:

$$\eta_c = 1.047 \cdot \exp(-0.0292 \cdot \beta) - 1.672 \cdot \exp(-0.5191 \cdot \beta) \quad (1)$$

Once the thermodynamic cycle is defined, dedicated sub-model for all the components that differ between the two schemes (evaporator heat exchangers) are implemented in order to find the geometry that allows the system operation according to the aforementioned cycle. Finally, performance and economic related parameters are obtained to perform the thermo-economic optimization.

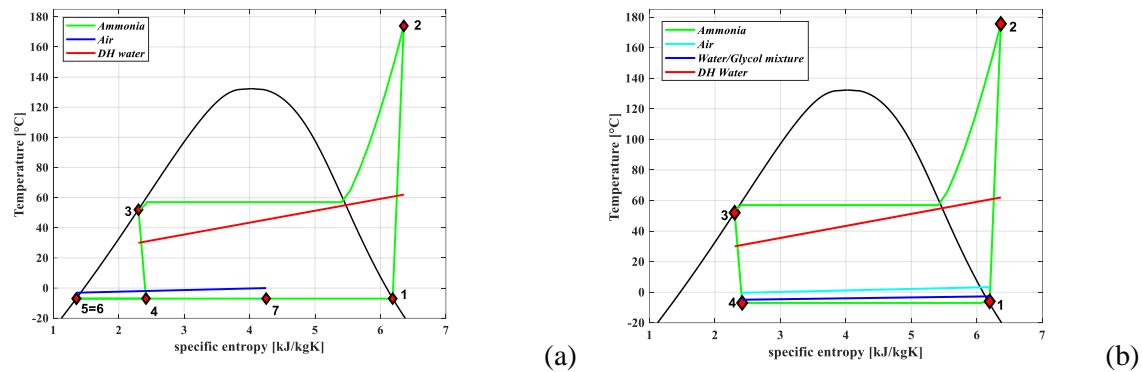


**Figure 2.** Direct expansion (a) and chilled water configuration (b) T-s diagram at condensation temperature,  $T_{co}$ , equal to 57 °C and evaporation temperature,  $T_{ev}$ , equal to -7 °C. The red line refers to district heating water temperature rise in the condenser from 30 °C to 62 °C.

### 3.2. Fin and tube heat exchangers: geometry definition and modelling

The evaporators and the heat collectors are wavy fin and tube heat exchangers. Ammonia, for the direct expansion solution and glycol/water mixture for the chilled water configuration pass inside several tubes arranged in rows, whereas air passes through the space among tubes and wavy fins, resulting in a counter-cross flow.

While copper ( $k = 390 \text{ Wm}^{-1}\text{K}^{-1}$ ) is employed for heat collector tubes, the evaporators tubes are made of stainless steel ( $k = 17 \text{ Wm}^{-1}\text{K}^{-1}$ ) due to the well-known compatibility problems between copper and ammonia. The material employed for wavy fins is aluminum ( $k = 230 \text{ Wm}^{-1}\text{K}^{-1}$ ).

Figure 3 shows schematic front and side views of the heat exchanger with the indication of all geometrical features that define an elementary unit.

The refrigerant flow is divided in several circuits in parallel in which the refrigerant mass flow rate is equally divided. According to this assumption, the heat transfer calculations will be performed iteratively only for one circuit, which has been divided in several elements where the heat rate is calculated as follows:

$$\delta\dot{Q} = U dA \Delta T_i \quad (2)$$

with the overall conductance of the element,  $U dA$ , evaluated as the sum of the convective internal tube resistance, conductive resistance and convective external surface one:

$$U dA = \frac{1}{\frac{1}{h_i d A_i} + \frac{s}{k d A} + \frac{1}{h_e d A_e}} \quad (3)$$

The internal convective heat transfer coefficient is calculated using specific correlations for single phase [7] or two-phase flows [8]. For the air side the model of Wang et. al for wavy fins [9] [10] is employed, considering also the dew formation on the tube [11]. The iterative calculation is performed

by integrating all the elements of the row (index  $j$ ) and then adding a row (index  $n$ ) as long as the total heat rate  $\dot{Q}$  reaches the design value  $\dot{Q}_{des}$ :

$$\dot{Q} = N_{circ} \sum_{n=1}^{N_r} \sum_{j=1}^{N_{el}} \delta \dot{Q}_{n,j} \geq \dot{Q}_{des} \quad (4)$$

The model takes into account a limit about the pressure drops on the refrigerant side in order to avoid large temperature glide that can impact in a negative way on the system performance. According to this, using Muller-Steinhagen and Heck correlation [12] for two-phase flow and Blasius equation for single-phase flow, the minimum number of circuits that respect the aforementioned limit is found.

*3.2.1. Fin and tube heat exchangers fans optimal choice.* Once the frontal air-side area, the volumetric flow rate  $\dot{V}_a$  and the pressure drop  $\Delta P$  across the rows are given, different types of axial fans configurations, in terms of rotor diameter  $D_{fan}$  and number of fans are evaluated to find the one with the lowest power consumption  $\dot{L}_{fan}$  and set-up costs. Using catalogue data, an Artificial Neural Network made up of one hidden layer with 20 neurons, working with the Levenberg-Marquardt algorithm has been trained. According to the expression below, the network takes as input the fan diameter, the air pressure drop and volumetric flow rate, and provides as output the fan rotating speed  $n_{fan}$ , the electrical power  $\dot{L}_{fan}$  and the sound pressure level  $L_{ps}$ :

$$D_{fan}, \Delta P, \dot{V}_a \rightarrow n_{fan}, \dot{L}_{fan}, L_{ps} \quad (5)$$

In particular, for each couple of volumetric flow rate and pressure drop values, fan diameters ranging from 650 to 1400 mm and a number of fans from 1 to 4 times the frontal air-side area aspect ratio (length over height ratio) have been tested.

### 3.3. Plate heat exchanger: geometry definition and modelling

The plate heat exchanger is used in the chilled water configuration as evaporator. Plates are made of stainless steel, having evaporating ammonia on one side and a glycol/water mixture on the other one. Since ammonia offers a huge latent heat, about 10 times greater than other typical refrigerant, there is a large difference in the flow rates between the two fluids, thus a multi-pass configuration on the refrigerant side is needed.

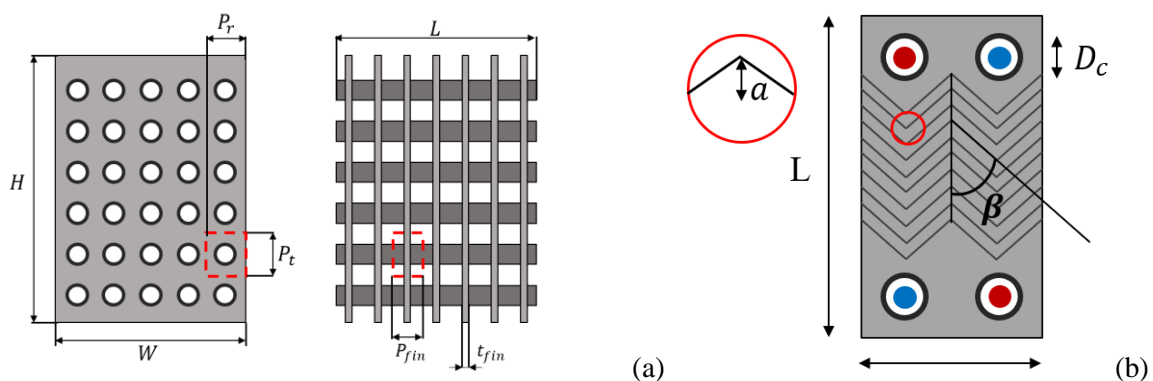


**Figure 3.** Fin and tube (a) and plate heat exchanger (b) geometrical features definition.

For this heat exchanger, the heat transfer computation is performed by dividing the single plate (figure 3) in several elements and, through an iterative calculation, temperature profiles and single

plate heat rate are obtained starting from the elementary heat rate calculated using equations (1) and (2), in which suitable heat transfer correlations are chosen for this geometry [13] [14]. Then, the total heat rate is equal to the single plate heat rate times the number of plates for each fluid.

### 3.4. Coefficient of performance and set-up costs evaluation

The coefficient of performance evaluation considers the condenser power  $\dot{Q}_{cond}$  as useful output and, as input, also the electrical power consumption of the auxiliary components such as fin and tube exchangers fans and glycol/water or refrigerant pump, as follows:

$$COP = \frac{\dot{Q}_{cond}}{\dot{I}_c + \dot{I}_{fan} + \dot{I}_{pump}} \quad (6)$$

The set-up costs calculation refers to an investment cost difference between the two systems proposed, based on the costs of the different components involved.

$$\Delta C_{set-up} = C_{hex} + C_{pump} + C_{fans} \quad (7)$$

The cost of heat exchanger  $C_{hex}$  refers to fin and tube type for the direct expansion solution and to the combination of fin and tube and plate heat exchangers for the chilled water configuration. All the component cost functions are shown in table 1. In order to highlight the cost impact of the different materials involved in the fin and tube heat exchangers, a cost function based on specific costs of materials instead of the heat exchange area is considered.

**Table 1.** Component cost functions.

Component	Cost function	Notes
Fin and tube heat exchanger [5]	$C_{steel/copper} \cdot m_{tubes} + C_{aluminum} \cdot m_{fans}$	
Plate heat exchanger [15]	$516.62 \cdot N_p \cdot W \cdot L + 268.45$	$W$ and $L$ in $m^2$
Axial fans [16]	$(1887.5 + 159.95 \cdot D^2 + 3.5343 \cdot D + 281.25 \cdot \dot{I}_{fan}) \cdot N_{fan}$	$\dot{I}_{fan}$ in $kW$ , $D$ in $m$
Pump [15]	$705.48 \cdot \dot{I}_{pump}^{0.71} \cdot \left(1 + \frac{0.2}{1 - \eta_p}\right)$	$\dot{I}_{pump}$ in $kW$

## 4. Resolution algorithm

The main steps of the algorithm used for the optimization can be resumed as follows:

- The thermodynamic cycle boundary conditions and all other variable data inputs are provided as shown in table 2.
- Fixed and variable geometrical inputs for the heat exchangers are defined as shown in table 3.
- All the thermodynamic cycle and heat exchangers variable data are combined together to obtain possible design solutions using all the models described in the previous part.
- For each solution, the optimal fan configuration choice through an optimization in terms of minimum power consumption and set-up costs is evaluated. In particular, the configuration with the minimum number of fans within a  $\pm 5\%$  relative distance from the configuration found with the utopia criterion was selected.
- Using the performance and economic parameters of all possible solutions, the optimal solution is found through a Pareto front analysis that seeks for the minimum total costs given by the sum of running and set-up costs.

## 5. Results

### 5.1. Operating parameters and constraints

Thermodynamic cycle and heat exchangers data used for the simulations are resumed in table 2 and 3. Also, two different average winter climate conditions for the same region (Denmark) have been considered as design boundary conditions: Aalborg ( $T_{amb} = 0\text{ }^{\circ}\text{C}$ ,  $\phi_{amb} = 85\%$ ) and Copenhagen ( $T_{amb} = -1\text{ }^{\circ}\text{C}$ ,  $\phi_{amb} = 75\%$ ). Thus, 4 design cases have been analysed (considering the two plant layouts and the two climatic conditions), each of them with a total number of solutions that is around  $1 \cdot 10^6$ . Among the thermodynamic cycle data, the constraint related to the refrigerant saturation temperature variation corresponding to the evaporator pressure drop is also varied. Instead, for the heat collectors there is a limit in water/glycol mixture velocity of  $4\text{ m} \cdot \text{s}^{-1}$ . As regards the plate heat exchanger, the elementary geometry is always fixed, and the model provides a sufficient number of plates to cope with the design heat rate.

**Table 2.** Thermodynamic cycle data.

Common fixed thermodynamic cycle data		Common variable thermodynamic cycle data	
Parameters	Value	Parameters	Range
Ambient temperature, $T_{amb}$ [ $^{\circ}\text{C}$ ]	5	Evaporator pinch point, $\Delta T_{pp,ev}$ [ $^{\circ}\text{C}$ ]	[1; 2; 3]
Relative humidity, $\phi_{amb}$ [%]	85	Air temperature variation, $\Delta T_a$ [ $^{\circ}\text{C}$ ]	[1; 2; 4; 6; 8]
Condensing temperature, $T_{cond}$ [ $^{\circ}\text{C}$ ]	57	Refrigerant temperature variation related to evaporator pressure drops, $\Delta T_g$ [ $^{\circ}\text{C}$ ]	[2; 3; 4]
Condensing power output, $\dot{Q}_{cond}$ [MW]	7.35	Heat collector pinch point [ $^{\circ}\text{C}$ ] <sup>b</sup>	[1; 2; 3]
Subcooling, $\Delta T_{sc}$ [ $^{\circ}\text{C}$ ]	5	Water/glycol mixture (50%) temperature variation, $\Delta T_w$ [ $^{\circ}\text{C}$ ] <sup>b</sup>	[4; 6; 8]
Pump overall efficiency, $\eta_p$	0.8	Evaporator outlet vapor quality, $x_7$ <sup>a</sup>	[0.2; 0.35; 0.5; 0.65]
Superheating, $\Delta T_{sh}$ [ $^{\circ}\text{C}$ ] <sup>b</sup>	5		

<sup>a</sup> Direct expansion configuration <sup>b</sup> Chilled water configuration

**Table 3.** Heat exchangers data.

Fin and tube heat exchanger fixed data		Plate heat exchanger fixed data	
Parameters	Value	Parameters	Value
Fin corrugation angle, $\theta$ [ $^{\circ}$ ]	10	Number of refrigerant passes, $n_p$	3
Height, $H$ [m]	[1.8 1.9 2]	Chevron angle, $\beta$ [ $^{\circ}$ ]	60
Fin and tube heat exchanger variable data		Corrugation depth, $a$ [mm]	0.9
Internal tube diameter, $d$ [mm]	[10 12.7 16]	Collector diameter, $D_c$ [mm]	300
Tube pitch, $P_t$ [mm]	From 40 to 55	Plate thickness, $t_p$ [mm]	2
Row pitch, $P_r$ [mm]	From 25 to 55	Plate pitch, $p_p$ [mm]	3
Fin pitch, $P_{fin}$ [mm]	[3 4 5]	Plate width, $W$ [mm]	1400
Fin thickness, $t_{fin}$ [mm]	[0.25 0.35]	Plate length, $L$ [mm]	3100
Air side frontal area aspect ratio, $F$	[1; 1.5; 2; 2.5; 3; 3.5; 4]		
Air velocity, $w_a$ [ $\text{ms}^{-1}$ ]	[1; 2; 3; 4]		

In order to avoid the possible oil retention in case of dry-out conditions in the direct expansion evaporators, all the simulations with an outlet vapor quality  $x_7$  greater than the dry-out vapor quality reduced by a factor of 20% that takes into account a potential refrigerant maldistribution inside tubes have been discarded.

About the fans possible configurations, all solutions with a sound pressure level beyond 85 dB(A) (measured at a distance of 1 m from the fan axis) or with a ratio between the fan diameter and the side of the squared fraction of the heat exchanger frontal area occupied by the fan lower than 0.5 or higher than 0.95 have been discarded.

## 5.2. Simulation results

The results for the two configurations in terms of COP and extra-cost of investment are shown in figure 4 for the Copenhagen case study. In particular, the best results are highlighted in blue, showing that the direct expansion configuration tends to have better performance than the chilled water one with always lower extra-cost of investment. From the performance point of view, this is due to higher evaporation temperature than the chilled water configuration for a fixed ambient air value, so the compressor power input  $\dot{L}_c$  is lower. In terms of investment costs, chilled water configuration is more expensive mainly because of the presence of the large size plate heat exchanger and also for copper-made tubes for the heat collectors which are more costly than stainless steel ones involved in fin and tube evaporators.

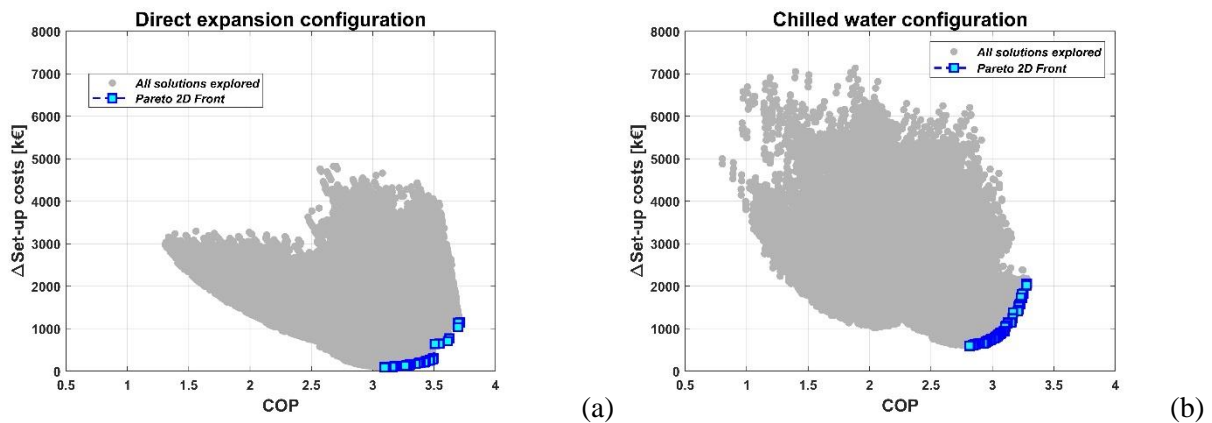


**Figure 4.** Pareto fronts for direct expansion (a) and chilled water configuration (b) for Copenhagen.

An economic analysis is performed, combining the extra-cost of investment presented above with the running costs, identifying a Pareto front and the optimal solution, as reported in figure 5 for both Aalborg and Copenhagen case study. The running costs  $RC$  are expressed as follows:

$$RC = \dot{Q}_{cond} \cdot COP^{-1} \cdot c_{en} \cdot h \quad [€] \quad (8)$$

In particular, to calculate the running costs three specific costs for the electricity  $c_{en}$  have been considered, equal to: 0.47, 0.24 and 0.09 € · kWh<sup>-1</sup> corresponding, respectively, to the average price of the electrical energy in the second half of 2022 [17], the 50% and 20% of the first value. The second and third values have been introduced as parameters, to explore a wide range of discount prices corresponding to self-production of the electricity (renewable sources, co-generation and similar options). Also,  $h$  is equal to 40000 hours, assuming a plant operational life of 10 years, with an average yearly amount of working hour equal to 4000.

The running costs are about ten times higher than the extra-costs of investment, so the optimal solution (highlighted with a golden star in figure 5) lies in the higher part of the front. According to the



different scenarios, the optimal solution changes. Indeed, the lower is the price of energy the lower is the performance, since the relative impact of the running costs on the optimal point choice becomes smaller.

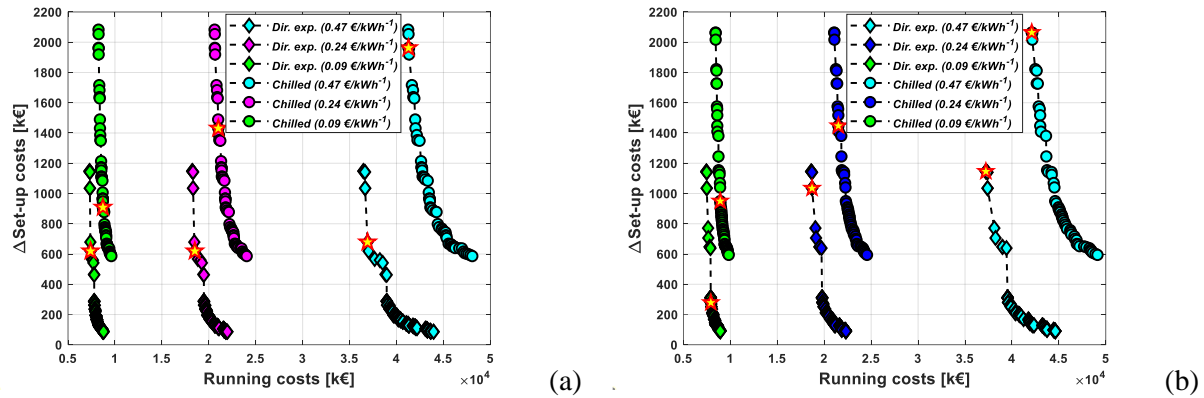


**Figure 5.** Comparison of the Pareto fronts for Aalborg (a) and Copenhagen (b) climatic conditions in the three running costs scenarios for both plant configurations.

About the fin and tube heat exchangers related to the optimal solutions, it is possible to notice that the direct expansion configurations have generally a higher number of modules instead of the chilled water one because of the smaller pinch-point and air temperature variation, leading to smaller modules in terms of number of rows.

**Table 4.** Results for optimal trade-off solutions in terms of set-up and running costs for the different scenarios assumed.

	Aalborg						Copenhagen					
	Direct expansion conf.			Chilled water conf.			Direct expansion conf.			Chilled water conf.		
$RC$ [ $\text{€kWh}^{-1}$ ]	0.47	0.24	0.09	0.47	0.24	0.09	0.47	0.24	0.09	0.47	0.24	0.09
COP	3.74	3.73	3.73	3.34	3.29	3.17	3.71	3.69	3.49	3.28	3.22	3.10
$\Delta C_{set-up}$ [k€]	679	619	619	1963	1431	908	1146	1035	279	2064	1447	950
$T_{ev}$ [ $^{\circ}\text{C}$ ]	-3	-3	-3	-9	-10	-11	-3	-3	-7	-10	-11	-12
$\dot{m}_{ev}^a; \dot{m}_w^b$	8.4	6.5	6.5	406	403	400	20.7	20.7	11.5	403	400	396
$x_7^a; \Delta T_w^b$	0.5	0.65	0.65	4	4	4	0.2	0.2	0.35	4	4	4
$\dot{Q}_{ev}$ [MW]	5.41	5.41	5.41	5.23	5.18	5.14	5.41	5.41	5.26	5.18	5.14	5.09
$\dot{L}_c$ [MW]	1.94	1.94	1.94	2.12	2.17	2.21	1.94	1.94	2.09	2.17	2.21	2.26
$\dot{L}_{fan}$ [kW]	23	29	29	30	20	27	38	47	13	31	29	32
$\dot{L}_{pump}$ [kW]	1.69	1.6	1.6	42	48	81	2.27	2.4	1.1	41	48	83
$\Delta T_{pp, ev}; \Delta T_{air}$	1; 2	1; 2	1; 2	2; 4	2; 4	3; 4	1; 1	1; 1	2; 4	2; 4	2; 4	3; 4
$N_{mod}$	308	279	279	184	137	165	520	466	125	198	148	168
$F$	1	1	1	2	2	1	1	1	1	2	2	1
$N_{row}$	1	1	1	6	4	3	1	1	1	6	4	3
$d$	16	16	16	16	12.7	16	16	16	16	16	12.7	16
$P_t; P_r$	40;55	40;55	40;55	40;55	40;40	40;55	40;55	40;55	40;55	40;55	40;40	45;55
$P_{fin}; t_{fin}$	3; 3.5	3; 3.5	3; 3.5	5; 2.5	3; 3.5	3; 2.5	3; 3.5	3; 3.5	3; 3.5	5; 2.5	3; 2.5	3; 3.5
$\dot{V}_a$ [ $\text{m}^3\text{h}^{-1}$ ]	11900	13040	13040	13870	14460	11580	11895	13040	13040	13870	15330	13550
$D_{fan}$ [mm]	1050	1000	1000	950	950	950	1050	1000	1000	950	950	950
$n_{fan}$ [rpm]	440	450	450	460	460	470	440	450	450	460	480	490
$N_{fan}$	1	1	1	2	2	1	1	1	1	2	2	1

<sup>a</sup> Direct expansion configuration <sup>b</sup> Chilled water configuration

Summary of symbols: direct expansion evaporators mass flow rate,  $\dot{m}_{ev}$ ; chilled water configuration heat collector water/glycol mixture flow rate  $\dot{m}_w$ ; total fans power consumption,  $\dot{L}_{fan}$ ; pump power consumption  $\dot{L}_{pump}$ ; total number of fin and tube modules  $N_{mod}$ ; number of circuits per row  $N_{row}$ ; number of fans per module  $N_{fan}$ .

Regarding the fans optimization, the minimum number of fans related to the aspect ratio is the common solution for all the highlighted points. This is due firstly to the strong influence of the number of fans on the cost function and secondly to a possible lower electric consumption of a single larger with respect to multiple smaller fans.

Therefore, there are some parameters changing considerably along the fronts, such as the number of modules (strongly related to pinch points and  $\Delta T_{air}$ ) and the evaporation temperature according to their significant impact on objective functions, instead of some other parameters such as tube and row pitches, fin pitch and thickness or  $\Delta T_w$  which are stabilized on common optimal values. Finally, Aalborg design case comes out as the best for both configurations in terms of performance due to the slightly more favorable climatic conditions than those of Copenhagen.

It is worth noting that the displayed optimal solutions should not be treated as absolute results, but strictly dependent on the specific cost functions employed.

## 6. Conclusions

In this work, a thermo-economic analysis of a 7.35 MW heat pump used for district heating purposes in the cities of Copenhagen and Aalborg (Denmark) was presented. Two different plant layouts with several thermodynamic cycle conditions and heat exchangers geometries were investigated in order to find the best solution in terms of running costs and extra-costs of investment for different scenarios. The analysis has shown that the direct expansion configuration is more convenient than the chilled water one for all the scenarios, with a decrease in performance of the optimal solutions when the specific cost of energy becomes smaller.

In this paper, only design conditions were investigated, and further analysis can be held on seasonal performances in order to calculate more detailed running costs, including a total environmental impact evaluation. Moreover, a safety assessment related to the system placement should be held in order to consider the higher risk for direct expansion configuration due to a higher ammonia charge.

## References

- [1] IEA (2022), Heating, IEA, Paris <https://www.iea.org/reports/heating>, License: CC BY 4.0.
- [2] European Environmental Agency (2022), <https://www.eea.europa.eu/ims/greenhouse-gas-emissions-from-energy>.
- [3] Gong Y, Ma G and Jiang Y 2023 *J Build Engin* **71** 106533.
- [4] Xiao S, Nefodov D, McLinden MO, Richter M and Urbaneck T 2022 *Solar Energy* **236** 499-511.
- [5] Citarella B, Viscito L, Mochizuki L and Mauro A W 2022 *Energy conv. and Manag.* **253** 115-52.
- [6] Botticella F, de Rossi F, Mauro A W, Vanoli G P and Viscito L 2018 *Int. J. Ref.* **87** 131-53.
- [7] Dittus F W and Boelter L M K, 1930 *Univ California Publ Eng.* **2**:443-61.
- [8] Gungor K and Winterton R H A 1986 *Int. J. Heat Mass Transfer* **29** 351-8.
- [9] Wang C C, Fu W L and Chang C T 1997 *Exp. Therm. Fl. Sc.* 174-186.
- [10] Wang C C, Jang J Y and Chiou N F 1999 *Int. J. Heat Mass Transfer* **42** 1919-1924.
- [11] Wang C C, Lin Y-T and Lee C-J 2000 *Int. J. Heat Mass Transfer* **43** 1869-72.
- [12] Müller-Steinhagen H and Heck K 1986 *Chem. Eng. and Process Process Intensif* **20** 297-308.
- [13] Martin H 1996 *Chem. Eng. Process.* **35** 301-310.
- [14] Amalfi R L, Vakili-Farahani F and Thome J R 2016 *Int. J. Ref.* **61** 185-203.
- [15] Pelella F, Zsembinszki G, Viscito L, Mauro A W and Cabeza L F 2023 *Appl. En.* **331** 120398.
- [16] Kashani A H A, Maddahi A and Hajabdollahi H 2013 *Appl. Therm. Eng.* **54** 43-55.
- [17] Statistics Denmark, <https://www.dst.dk/en/Statistik/emner/miljoe-og-energi/energiforbrug-og-energipriser/energipriser>.